

Nuclear physics with *TriSol* at Notre Dame's Nuclear Science Laboratory

T. Ahn ^{*}, D.W. Bardayan, D. Blankstein, C. Boomershine, M. Brodeur, S. Carmichael, S. Coil, J.J. Kolata, P.D. O'Malley, W. Porter, J.S. Randhawa, F. Rivero, J. Rufino, W.W. von Seeger, R. Zite

Department of Physics and Astronomy, University of Notre Dame, 225 Nieuwland Science Hall, Notre Dame, IN 46556, USA



ARTICLE INFO

Keywords:
Radioactive beams
Solenoid spectrometer

ABSTRACT

The detailed study of radioactive nuclei has resulted in opportunities for addressing many open questions in low-energy nuclear physics. For over three decades, the *TwinSol* separator at the University of Notre Dame has produced high-quality in-flight radioactive beams at low-energy for light isotopes that have been used in experiments aimed at nuclear structure, astrophysics, and fundamental symmetries studies. We have recently upgraded the *TwinSol* separator by adding additional elements: a dipole magnet, and a third solenoid. This new *TriSol* separator will improve the quality and purity of future radioactive beams. This improvement will enable the use of heavier beams and address beam contamination that has hindered past experiments. The current status of *TriSol* and its science program will be presented along with the role the *TriSol* program plays in the current landscape of nuclear physics user facilities. The *TriSol* program includes plans for studies of $^{11}\text{C}(p, p)^{11}\text{C}$ reaction for investigating the nature of the first stars, $^{14}\text{O}(\alpha, p)^{17}\text{F}$ and its influence on reaction networks in X-ray bursts, the measurement of fusion reactions on Ne isotopes important for pycnonuclear reactions, precision half-life measurements for fundamental symmetries studies, and the use of *TriSol* as a magnetic spectrometer.

1. Introduction

TwinSol [1] is a separator that has been used for producing in-flight radioactive beams at Notre Dame's Nuclear Science Laboratory (NSL). It consists of two superconducting solenoids that are used to refocus one of several reaction products to produce a secondary beam. *TwinSol* can produce secondary beams one or two nucleons from stability for a large range of radioactive nuclei in the $A \approx 3 - 40$ mass region.

One of the advantages of *TwinSol* is its large angular acceptance of reaction products. The use of two solenoids instead of one enables more constraints for the transmission of the reaction products resulting in a higher degree of separation of unwanted products and the secondary beam of interest. A natural extension of this concept is the addition of ion-optical elements such as a third solenoid. This is what we have done with *TriSol*, extending *TwinSol* with a dipole magnet and third superconducting solenoid magnet. These additional elements allow for a higher degree of separation and thus higher quality radioactive beams. The details of *TriSol* and its commissioning including the simulation of secondary beams and the measurements confirming the simulations are given in Ref. [2].

In the landscape of radioactive beam facilities worldwide, the University of Notre Dame's NSL offers experiments that are complementary

to laboratories that use higher energies for their radioactive beam production. At the NSL, *TriSol*'s unique advantage is the production of high-quality radioactive beams near stability at low energy in the range of about 1–5 MeV/u. *TriSol*'s radioactive beams enable a wide range of studies in nuclear structure, reactions, and astrophysics near the Coulomb barrier. Specific examples include investigations of the nuclear structure of light unstable nuclei, fusion barriers, classical novae, X-ray bursts, pycnonuclear reactions, and tests of the Standard Model. In the following section, we will present some details and simulations of *TriSol*. In Section 3, we will present currently planned measurements with *TriSol*.

2. *TriSol* simulation and optimization

TriSol consists of a primary production target, the first solenoid, a crossover point with an iris, a second solenoid, a dipole magnet, a third solenoid, and a secondary target. The new dipole magnet and third solenoid were installed in 2021 and fully commissioned in 2022. Additional details on the results of the first tests can be found in Ref. [2]. The additional ion-optical elements allow for a greater degree of selectivity and focusing, which were characterized well with simulations with the

^{*} Corresponding author.

E-mail address: tan.ahn@nd.edu (T. Ahn).

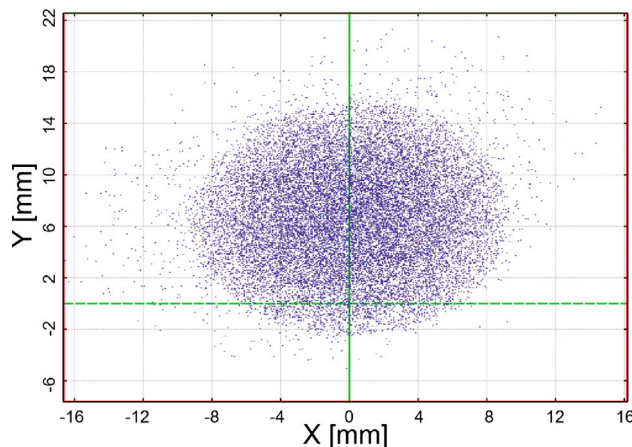


Fig. 1. LISE++ calculation of the transmission of the radioactive beam ^{17}F produced by the $^{16}\text{O}(d, n)^{17}\text{F}$ reaction.

transport program LISE++ [3]. The switching magnet also allows for the permanent installation of the St. Benedict ion trapping system next to *TriSol*.

The additional elements allow for reduced beam spot size in many situations, which will benefit many experiments. A typical reduction in FWHM radius is from 25 mm to 8 mm, which is much better suited for reaction studies. A plot of the simulated spot size of a ^{17}F beam produced by *TriSol* in the $^{16}\text{O}(d, n)^{17}\text{F}$ reaction is shown in Fig. 1. Although the initial commissioning of *TriSol* has been completed, continual characterizations and adjustments are being performed to optimize the final beam. In Fig. 1, it can be seen that the beam is slightly off center and 6 mm high. The level of detail given by the LISE++ calculations allows us to understand the origin of this result and compensate for small misalignments. Additionally, simulations indicate separation between ^{17}F and the primary ^{16}O beam can be achieved using a thin carbon stripping foil at the crossover point between the first two solenoids. It has been found that introducing a $50 \mu\text{g}/\text{cm}^2$ carbon foil for the ^{17}F beam can change the charge state from 8^+ to 9^+ and cleanly separate it from the primary ^{16}O beam.

3. Future planned experiments

With the additional selectivity of *TriSol*, there are a number of now-enabled experiments that are planned for the near future. There are also a number of new and developing instruments that will complement and take full advantage of the available *TriSol* beams that will be highlighted in the examples below.

3.1. $^{11}\text{C}(p, p)^{11}\text{C}$

Primordial stars are thought to have been very massive and short lived. These stars initially consist of very light ingredients such as hydrogen and helium that are synthesized into heavier elements such as carbon, nitrogen, and oxygen. In very old stars, we see that some of them have an enhancement of carbon, oxygen, and/or nitrogen but are poor in elements heavier than these. This indicates that helium burning may have played a role in primordial stars. As the primordial stars are thought to be more massive than second-generation stars, they will burn via the hot pp -chain and the triple- α process [4,5]. The α -capture reactions on ^7Be and proton-capture reactions on ^{11}C are identified as being the most important in understanding reactions in the primordial stars, but radioactive beams are required for the study of these reactions and data for these are sparse.

One possible reaction chain of importance for the production of elements such as carbon is the $^7\text{Be}(\alpha, \gamma)^{11}\text{C}(p, \gamma)^{12}\text{N}$ chain. There are

indications that the cross section for the $^{11}\text{C}(p, \gamma)^{12}\text{N}$ reaction may be large as indicated by transfer and knock-out reaction studies [6,7]. We plan to use *TriSol* to produce a high-quality ^{11}C beam at low energy with an approximate intensity of $10^5\text{--}10^6$ pps to measure the $^{11}\text{C}(p, p)^{11}\text{C}$ reaction, which will be an important step for constraining the $^{11}\text{C}(p, \gamma)^{12}\text{N}$ reaction.

3.2. Fusion experiments in the Mg and Ne region

A number of nuclear reactions play a pivotal role in phenomena associated with neutron stars, the most dense form of matter in the universe outside of black holes. One of these phenomena is Type Ia X-ray bursts. Type Ia X-ray bursts are events where accreted hydrogen from a neutron star's companion star accumulates and then ignites on the surface of the neutron star [8]. This ignition is due to the heating of the accreted material and the subsequent thermonuclear runaway is powered by a network of nuclear reactions. The deep gravitational potential of the neutron star does not allow for the ignition products to escape but rather they are accumulated back on the surface where they migrate lower into the neutron star crust. Due to the extreme pressures inside the crust, the nuclei from the ashes of the reactions are confined to a crystal lattice with very small spacing where the nuclei may fuse due to their proximity and zero-point oscillations [9]. These reactions, called pycnonuclear reactions, may contribute additional thermal energy to the crust and can affect the rate of cooling of the surface. Our understanding of theoretical cooling curves must be compared with what is observed by X-ray observatories.

Reaction network calculations indicate that the region around neutron-rich Ne isotopes is important for determining the energy generation of pycnonuclear reactions [9]. There is currently a dearth of information on fusion cross sections at low energy even for stable Ne isotopes. In order to experimentally constrain the relevant fusion reaction cross sections, we plan to study the $^{24,26}\text{Mg} + ^{20}\text{Ne}$ fusion reaction at the lowest energy cross sections that we can measure using the ND-Cube active-target detector [10]. The ND-Cube will allow for the use of a Ne target and will yield high-resolution position information, which translates into high energy resolution. Recent developments with Ne:H₂ gas mixtures allow for the use of multi-layer thick Gas Electron Multipliers (Th-GEM) for the amplification of electron signals with relatively low gas pressures. The use of a small amount of H₂ has been shown to reduce sparking and increase gains over pure Ne [11], which will allow for a large amount of small electrodes that enable the high position resolution.

Preliminary measurements have been performed for the $^{24,26}\text{Mg} + ^{20}\text{Ne}$ fusion reactions at various positions of the *TriSol* beamline as it was being constructed. The ^{26}Mg experiment was performed with the ND-Cube placed in the position that will be used for future radioactive beams, downstream of the third solenoid. A photograph of the ND-Cube coupled to the third solenoid is shown in Fig. 2. The ND-Cube was filled with about 200 Torr of a Ne:H₂ gas mixture in a (95:5) ratio. Beams of ^{24}Mg and ^{26}Mg were used in two separate measurements at 80 MeV and 81 MeV, respectively. Preliminary results show that we are able to successfully image the beam tracks in the ND-Cube. In Fig. 3, events for the $^{24}\text{Mg} + ^{20}\text{Ne}$ measurement are shown, where a reconstructed beam image is given as black squares and three shorter-track events are shown as blue, green, and red circles. Track length and charge density can be used to uniquely identify fusion events. These preliminary runs have been completed and our goal is to characterize the position and energy resolution and optimize experimental parameters for measurements for the lowest cross sections we can measure.

Future experiments will include producing an in-flight ^{20}Ne secondary beam through the proton-adding $^{19}\text{F}(^3\text{He}, d)^{20}\text{Ne}$ reaction. The use of *TriSol* allows us to overcome the limitation of not being able to accelerate noble gases with the FN Tandem Van de Graaff. $^{20}\text{Ne} + ^{20}\text{Ne}$ reactions will be the stepping stone to measurements with neutron-rich Mg and Ne isotopes at radioactive beam user facilities.

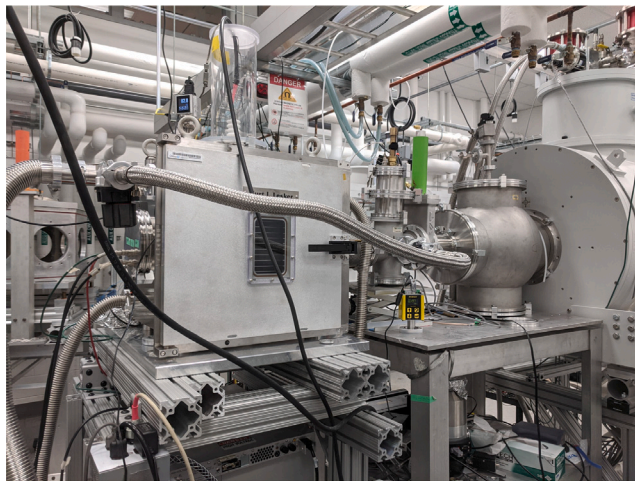


Fig. 2. Photograph of the ND-Cube attached to the *TriSol* beamline downstream of the third solenoid.

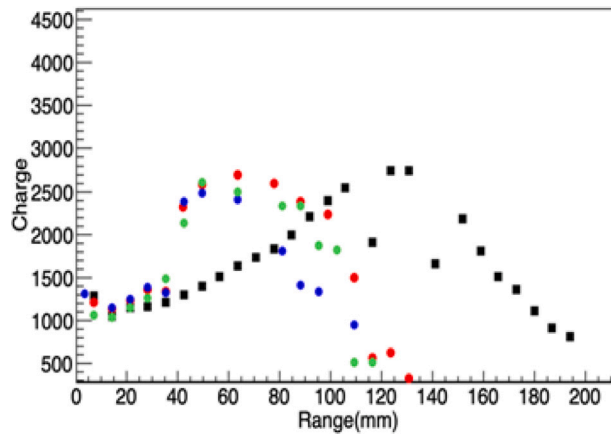


Fig. 3. A beam event (black squares) and three shorter tracks (blue, green, and red circles) from $^{24}\text{Mg} + ^{20}\text{Ne}$ fusion experiment are shown.

3.3. $^{14}\text{O}(\alpha, p)^{17}\text{F}$

One of the most important reactions that governs the αp process is the $^{14}\text{O}(\alpha, p)^{17}\text{F}$ reaction that are important for understanding events such as Type Ia X-ray bursts [12,13]. This reaction can be studied directly with a radioactive ^{14}O beam, but previous attempts were limited in success due to the large degree of contamination of the secondary beam. With *TriSol*, the additional ion-optical elements allow for a cleaner separation of ^{14}O enabling the measurement at the NSL.

A newly commissioned active-target detector, ATHENA [14], is planned to be used for the study of the $^{14}\text{O}(\alpha, p)^{17}\text{F}$ reaction. ATHENA has been used to study $\text{Mg} + \alpha$ reactions. The sensitivity to reaction cross sections has shown that $^{25,26}\text{Mg}(\alpha, n)^{28,29}\text{Si}$ reactions can be measured and separated from competing (α, α) reactions [15]. A plot of the energy loss vs. energy (Fig. 4) shows the degree of separation of (α, n) and (α, α') reactions, the later having a relatively larger cross section. Similarly, ATHENA will allow for the $^{14}\text{O}(\alpha, p)^{17}\text{F}$ reaction inclusive cross section to be measured for a range of energies. However, due to ATHENA's rate limitations, the time-inverse reaction, $^{17}\text{F}(p, \alpha)^{14}\text{O}$ will be measured with a thin CH_2 target for the lowest energies.

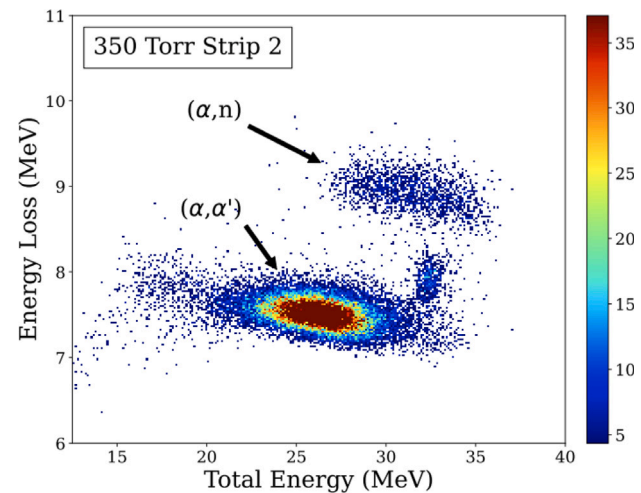


Fig. 4. A plot of energy loss vs. energy for the $^{26}\text{Mg} + ^4\text{He}$ measurement for reactions in the second strip of ATHENA with 350 Torr of helium gas. This shows a clear separation of the (α, n) and (α, α') channels.

3.4. Fundamental symmetries: Half-life measurements

A number of precision half-life measurements have been performed for studies in fundamental symmetries using radioactive beams from *TwinSol*. The current 3σ tension with unitarity of the CKM matrix [16] resulting from recent transition-independent radiative correction calculations [17–20] has triggered a surge in experimental and theoretical efforts to put the determination of the V_{ud} element of that matrix on a more solid footing. One such effort consist of obtaining V_{ud} from super-allowed mixed decays between mirror nuclei [21]. A central ingredient in this determination is the precise knowledge of the ft-value of the decay and it was found that for several transitions, the uncertainty on that quantity was dominated by imprecise and sometimes inaccurate half-lives [22]. Hence in the past several years several precision half-life measurements have been performed using *TwinSol* beams including the recent half-life measurements of ^{29}P [23], ^{13}N [24], and ^{15}O [25]. These half-life measurements are performed by implantation of the radioactive isotope of interest into a gold foil, which is then rotated periodically in front of a plastic-scintillator counter [24]. A key ingredient of the success of these measurements is the precise characterization of any potential contaminants that are present in the final target. Due to the high precision required for improving the limits on future half-life measurements, even a small amount of contaminant with a similar lifetime can skew the final results. *TriSol*'s improved selectivity will allow for half-life measurements that were previously hampered by contaminants as well as achieving beam purities where the heaviest secondary beams produced at the NSL will become viable. Future planned measurements that will be enabled by *TriSol* includes ^{19}Ne , ^{23}Mg , ^{31}S , and ^{41}Sc . Furthermore, the 3rd solenoid will enable the production of tertiary beams of otherwise difficult to produce isotopes such as ^{21}Na , which half-life suffers from conflicting measurements [26].

3.5. Use of *TriSol* as a spectrometer: Study of ^{19}Ne

A novel implementation of *TriSol* is to use its magnets as a spectrometer. Before the commissioning of *TriSol*, this idea was first performed with the *TwinSol*'s solenoid magnets to study levels in ^{19}Ne that are important for constraining the $^{15}\text{O}(\alpha, \gamma)^{19}\text{Ne}$ reaction. This reaction is thought to be the main breakout reaction for the hot-CNO cycle in the αp process and therefore has implications for our understanding of X-ray bursts [27]. To study the levels in ^{19}Ne , we used the

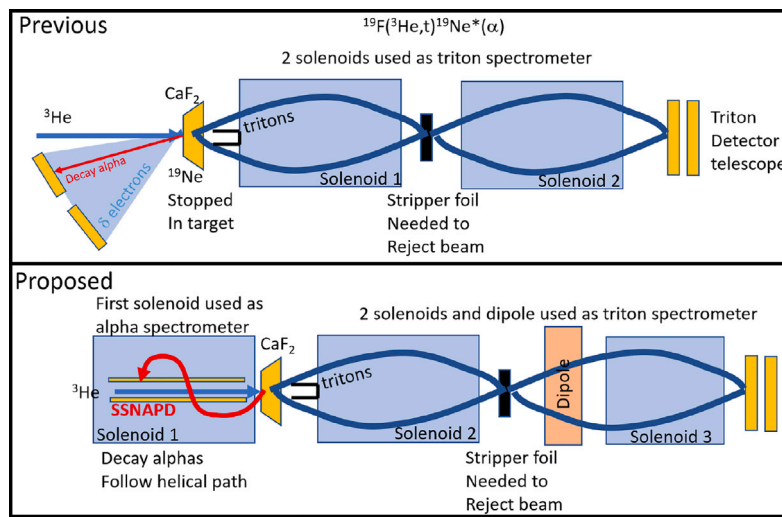


Fig. 5. An illustration of using *TriSol* as a spectrometer to refocus outgoing reaction products. The first solenoid will be used to momentum analyze outgoing α particles in a device called SSNAPD.

$^{19}\text{F}({}^3\text{He}, t)^{19}\text{Ne}$ reaction where the outgoing tritons were refocused by the two *TwinSol* solenoids and sent into a Si detector at the secondary focus [27]. The experimental setup is shown in Fig. 5 (top). This measurement with *TwinSol* gave the first experimental rate for the $^{15}\text{O}(\alpha, \gamma)^{19}\text{Ne}$ reaction through the measurement of the α -decay branching ratio. With *TriSol*, the limitations of the previous experiment due to background can be overcome by using an additional solenoid to magnetically analyze the outgoing α particles from ^{19}Ne . This new spectrometer, the Solenoid Spectrometer for Nuclear Astrophysics and Decays (SSNAPD), is currently under development and shown in Fig. 5 (bottom). Results from a prototype of SSNAPD can be found in Ref. [28]. SSNAPD with *TriSol* will allow for measurements of the α branching ratio measurement with a precision of one part in 10^{-5} . SSNAPD will also be used with other reactions to detect protons, deuterons, and α particles for studies in nuclear structure and astrophysics such as clusters in light nuclei and (p, γ) reactions.

4. Summary and outlook

The successful research program of *TwinSol* over the last two and half decades has paved the way for improving experiments by developing *TriSol*, which will provide higher quality radioactive beams. The improved purity and focusing of the secondary beams allows for many more experiments near the Coulomb barrier that are relevant for nuclear structure, reactions, astrophysics, and fundamental symmetries. Many examples of future experiments were given in this paper, which highlights the possibilities with the suite of instruments that can be coupled to *TriSol*.

Declaration of competing interest

The authors declare that they have no known competing financial interests or personal relationships that could have appeared to influence the work reported in this paper.

Acknowledgments

This work was supported by the U.S. National Science Foundation, United States Grant No's. PHY-2011890 and 2117687 and the University of Notre Dame, United States.

References

- [1] F. Becchetti, M. Lee, T. O'Donnell, D. Roberts, J. Kolata, L. Lamm, G. Rogachev, V. Guimarães, P. DeYoung, S. Vincent, Nucl. Instrum. Methods Phys. Res. A 505 (1–2) (2003) 377–380, [http://dx.doi.org/10.1016/S0168-9002\(03\)01101-X](http://dx.doi.org/10.1016/S0168-9002(03)01101-X), URL <http://linkinghub.elsevier.com/retrieve/pii/S016890020301101X>.
- [2] P.D. O'Malley, T. Ahn, D.W. Bardayan, M. Brodeur, S. Coil, J.J. Kolata, Nucl. Instrum. Methods Phys. Res. A 1047 (2023) 167784, <http://dx.doi.org/10.1016/J.NIMA.2022.167784>.
- [3] O.B. Tarasov, D. Bazin, Nucl. Instrum. Methods Phys. Res. B (2008) <http://dx.doi.org/10.1016/j.nimb.2008.05.110>.
- [4] O. Clarkson, F. Herwig, M. Pignatari, Mon. Not. R. Astron. Soc.: Lett. 474 (1) (2018) L37–L41, <http://dx.doi.org/10.1093/MNRASL/SLX190>, URL <https://academic.oup.com/mnrasl/article/474/1/L37/4655185>, arXiv:1710.01763.
- [5] M. Wiescher, O. Clarkson, R.J. DeBoer, P. Denisenkov, Eur. Phys. J. A 57 (1) (2021) 1–11, <http://dx.doi.org/10.1140/EPJA/S10050-020-00339-X>, URL <https://link.springer.com/article/10.1140/epja/s10050-020-00339-X>.
- [6] X. Tang, A. Azhari, C.A. Gagliardi, A.M. Mukhamedzhanov, F. Pirlepesov, L. Trache, R.E. Tribble, V. Burjan, V. Kroha, F. Carstoiu, Phys. Rev. C 67 (1) (2003) 015804, <http://dx.doi.org/10.1103/PhysRevC.67.015804>, URL <https://journals.aps.org/prc/abstract/10.1103/PhysRevC.67.015804>.
- [7] L.G. Sobotka, W.W. Buhro, R.J. Charity, J.M. Elson, M.F. Jager, J. Manfredi, M.H. Mahzoon, A.M. Mukhamedzhanov, V. Eremenko, M. McCleskey, R.G. Pizzone, B.T. Roeder, A. Spiridon, E. Simmons, L. Trache, M. Kurokawa, P. Navrátil, Phys. Rev. C - Nucl. Phys. 87 (5) (2013) 054329, <http://dx.doi.org/10.1103/PHYSREVC.87.054329/FIGURES/7/MEDIUM>, URL <https://journals.aps.org/prc/abstract/10.1103/PhysRevC.87.054329>.
- [8] A. Parikh, J. José, G. Sala, C. Iliadis, Nucleosynthesis in type I X-ray bursts, 2013, pp. 225–253, <http://dx.doi.org/10.1016/j.pnpp.2012.11.002>, arXiv:1211.5900.
- [9] Z. Meisel, A. Deibel, L. Keek, P. Shternin, J. Elfritz, J. Phys. G: Nucl. Part. Phys. 45 (9) (2018) 093001, <http://dx.doi.org/10.1088/1361-6471/AAD171>, URL <https://iopscience-iop-org.proxy.library.nd.edu/article/10.1088/1361-6471/aad171>, <https://iopscience-iop-org.proxy.library.nd.edu/article/10.1088/1361-6471/aad171/meta>, arXiv:1807.01150.
- [10] T. Ahn, J.S. Randhawa, S. Aguilar, D. Blankstein, L. Delgado, N. Dixneuf, S.L. Henderson, W. Jackson, L. Jensen, S. Jin, J. Koci, J.J. Kolata, J. Lai, J. Levano, X. Li, A. Mubarak, P.D. O'Malley, S. Ramirez Martin, M. Renaud, M.Z. Serikow, A. Tollefson, J. Wilson, L. Yan, Nucl. Instrum. Methods Phys. Res. A 1025 (2022) 166180, <http://dx.doi.org/10.1016/J.NIMA.2021.166180>, arXiv:2106.13236.
- [11] J.S. Randhawa, T. Ahn, J.J. Kolata, P. O'Malley, A. Ontiveros, Nucl. Instrum. Methods Phys. Res. A 1041 (2022) 167256, <http://dx.doi.org/10.1016/J.NIMA.2022.167256>.
- [12] A. Parikh, J. José, F. Moreno, C. Iliadis, Astrophys. J. Suppl. Ser. 178 (1) (2008) 110–136, <http://dx.doi.org/10.1086/589879>, URL <http://stacks.iop.org/0067-0049/178/i=1/a=110>.
- [13] R.H. Cyburt, A.M. Amthor, A. Heger, E. Johnson, L. Keek, Z. Meisel, H. Schatz, K. Smith, Astrophys. J. 830 (2) (2016) 55, <http://dx.doi.org/10.3847/0004-637X/830/2/55>, URL <http://stacks.iop.org/0004-637X/830/2/a=55?key=crossref.fbca44ebd1aaa63d911014d9d3dd7792>.

[14] D. Blankstein, D.W. Bardayan, J.M. Allen, C. Boomershine, L.K. Callahan, S. Carmichael, S.L. Henderson, P.D. O’Malley, Nucl. Instrum. Methods Phys. Res. A 1047 (2023) 167777, <http://dx.doi.org/10.1016/J.NIMA.2022.167777>.

[15] D. Blankstein, Active Target Measurement Of the $^{25,26}\text{Mg}(\alpha,\text{n})^{28,29}\text{Si}$ Total Cross section (Ph.D. thesis), University of Notre Dame, 2023.

[16] V. Cirigliano, A. Crivellin, M. Hoferichter, M. Moulson, Phys. Lett. B 838 (2023) 137748, <http://dx.doi.org/10.1016/j.physletb.2023.137748>, URL <http://arxiv.org/abs/2208.11707>. arXiv:2208.11707.

[17] C.Y. Seng, M. Gorchtein, H.H. Patel, M.J. Ramsey-Musolf, Phys. Rev. Lett. 121 (24) (2018) 241804, <http://dx.doi.org/10.1103/PHYSREVLETT.121.241804/FIGURES/5/MEDIUM>, URL <https://journals.aps.org/prl/abstract/10.1103/PhysRevLett.121.241804>. arXiv:1807.10197.

[18] A. Czarnecki, W.J. Marciano, A. Sirlin, Phys. Rev. D 100 (7) (2019) 073008, <http://dx.doi.org/10.1103/PHYSREVD.100.073008/FIGURES/4/MEDIUM>, URL <https://journals.aps.org/prd/abstract/10.1103/PhysRevD.100.073008>. arXiv:1907.06737.

[19] C.Y. Seng, X. Feng, M. Gorchtein, L.C. Jin, Phys. Rev. D 101 (11) (2020) 111301, <http://dx.doi.org/10.1103/PHYSREVD.101.111301/FIGURES/5/MEDIUM>, URL <https://journals.aps.org/prd/abstract/10.1103/PhysRevD.101.111301>.

[20] K. Shiells, P.G. Blunden, W. Melnitchouk, Phys. Rev. D 104 (3) (2021) 033003, <http://dx.doi.org/10.1103/PHYSREVD.104.033003/FIGURES/10/MEDIUM>, URL <https://journals.aps.org/prd/abstract/10.1103/PhysRevD.104.033003>.

[21] O. Naviliat-Cuncic, N. Severijns, Phys. Rev. Lett. 102 (14) (2009) 142302, <http://dx.doi.org/10.1103/PHYSREVLETT.102.142302/FIGURES/1/MEDIUM>, URL <https://journals.aps.org/prl/abstract/10.1103/PhysRevLett.102.142302>.

[22] N. Severijns, M. Tandekci, T. Phalet, I.S. Towner, Phys. Rev. C - Nucl. Phys. 78 (5) (2008) 055501, <http://dx.doi.org/10.1103/PHYSREVC.78.055501/FIGURES/1/MEDIUM>, URL <https://journals.aps.org/prc/abstract/10.1103/PhysRevC.78.055501>.

[23] J. Long, M. Brodeur, M. Baines, D.W. Bardayan, F.D. Becchetti, D. Blankstein, C. Boomershine, D.P. Burdette, A.M. Clark, B. Frentz, S.L. Henderson, J.M. Kelly, J.J. Kolata, B. Liu, K.T. Macon, P.D. O’Malley, A. Pardo, C. Seymour, S.Y. Strauss, B. Vande Kolk, Phys. Rev. C 101 (1) (2020) 015501, <http://dx.doi.org/10.1103/PHYSREVC.101.015501/FIGURES/9/MEDIUM>, URL <https://journals.aps.org/prc/abstract/10.1103/PhysRevC.101.015501>.

[24] J. Long, C.R. Nicoloff, D.W. Bardayan, F.D. Becchetti, D. Blankstein, C. Boomershine, D.P. Burdette, M.A. Caprio, L. Caves, P.J. Fasano, B. Frentz, S.L. Henderson, J.M. Kelly, J.J. Kolata, B. Liu, P.D. O’Malley, S.Y. Strauss, R. Zite, M. Brodeur, Phys. Rev. C 106 (4) (2022) 045501, <http://dx.doi.org/10.1103/PHYSREVC.106.045501/FIGURES/11/MEDIUM>, URL <https://journals.aps.org/prc/abstract/10.1103/PhysRevC.106.045501>.

[25] D.P. Burdette, M. Brodeur, D.W. Bardayan, F.D. Becchetti, D. Blankstein, C. Boomershine, L. Caves, S.L. Henderson, J.J. Kolata, B. Liu, J. Long, P.D. O’Malley, S.Y. Strauss, Phys. Rev. C 101 (5) (2020) 055504, <http://dx.doi.org/10.1103/PHYSREVC.101.055504/FIGURES/11/MEDIUM>, URL <https://journals.aps.org/prc/abstract/10.1103/PhysRevC.101.055504>.

[26] N. Severijns, L. Hayen, V. De Leebeeck, S. Vanlangendonck, K. Bodek, D. Rozpedzik, I.S. Towner, Phys. Rev. C 107 (1) (2023) 015502, <http://dx.doi.org/10.1103/PHYSREVC.107.015502/FIGURES/23/MEDIUM>, URL <https://journals.aps.org/prc/abstract/10.1103/PhysRevC.107.015502>.

[27] W.P. Tan, J.L. Fisker, J. Görres, M. Couder, M. Wiescher, Phys. Rev. Lett. 98 (24) (2007) 242503, <http://dx.doi.org/10.1103/PHYSREVLETT.98.242503/FIGURES/5/MEDIUM>, URL <https://journals.aps.org/prl/abstract/10.1103/PhysRevLett.98.242503>.

[28] J. Allen, P.D. O’Malley, N. Applegate, D.W. Bardayan, D. Blankstein, M.R. Hall, O. Hall, J.J. Kolata, F.D. Becchetti, Nucl. Instrum. Methods Phys. Res. A 954 (2020) 161350, <http://dx.doi.org/10.1016/J.NIMA.2018.10.028>.